Molecular and functional assessment of multicellular cancer spheroids produced in double emulsions enabled by efficient airway resistance based selective surface treatment

OPEN ACCESS
IOP Publishing
Journal of Micromechanics and Microengineering
J. Micromech. Microeng. **27** (2017) 095014 (9pp)
https://doi.org/10.1088/1361-6439/aa7e92

Molecular and functional assessment of multicellular cancer spheroids produced in double emulsions enabled by efficient airway resistance based selective surface treatment

Xiao Ma[1,2], Morten Leth Jepsen[1,2], Anne Kathrine R Ivarsen[3], Birgitta R Knudsen[1,2] and Yi-Ping Ho[4]

[1] Interdisciplinary Nanoscience Center (iNANO), Aarhus University, Aarhus, Denmark
[2] Department of Molecular Biology and Genetics, Aarhus University, Aarhus, Denmark
[3] Department of Engineering, Aarhus University, Aarhus, Denmark
[4] Department of Biomedical Engineering, The Chinese University of Hong Kong, Shatin, NT, Hong Kong SAR, People's Republic of China

E-mail: ypho@cuhk.edu.hk

Received 12 May 2017, revised 27 June 2017
Accepted for publication 10 July 2017
Published 22 August 2017

Abstract

Multicellular spheroids have garnered significant attention as an *in vitro* three-dimensional cancer model which can mimick the *in vivo* microenvironmental features. While microfluidics generated double emulsions have become a potential method to generate spheroids, challenges remain on the tedious procedures. Enabled by a novel 'airway resistance' based selective surface treatment, this study presents an easy and facile generation of double emulsions for the initiation and cultivation of multicellular spheroids in a scaffold-free format. Combining with our previously developed DNA nanosensors, intestinal spheroids produced in the double emulsions have shown an elevated activities of an essential DNA modifying enzyme, the topoisomerase I. The observed molecular and functional characteristics of spheroids produced in double emulsions are similar to the counterparts produced by the commercially available ultra-low attachment plates. However, the double emulsions excel for their improved uniformity, and the consistency of the results obtained by subsequent analysis of the spheroids. The presented technique is expected to ease the burden of producing spheroids and to promote the spheroids model for cancer or stem cell study.

Keywords: spheroids, topoisomerase, double emulsions, microfluidics, surface treatment

Supplementary material for this article is available online

(Some figures may appear in colour only in the online journal)

Introduction

Mounting evidence has suggested that the cell-to-cell interactions and extracellular matrix (ECM) mechanics are distinctively different, when cells are interacting in a three-dimensional (3D) architecture as opposed to in conventional two-dimensional (2D) cell cultures [1]. Cellular adhesion and ECM not only serve as physical scaffolds to support the tissues three-dimensionally, but also trigger different receptors and signalling pathways [2, 3] that subsequently mediate cellular survival and differentiation. For example, impaired interaction of the cells with ECM, mediated by tight junction proteins and cell adhesion molecules such as β1 integrins [4] and E-cadherin [5], may result in different cell phenotypes. Furthermore, mechanical stress that acts upon the cells and alters the ECM signalling, has also shown detrimental for the control of gene-expression, as well as in the determination of cell fates [6, 7].

In accordance with the recognition that 2D cell cultures lack the adequate cell–cell interactions and ECM presented in the human tissues, 3D cell culture models have gained growing interest for the studies of tumours and tissue engineering due to their obvious advantages of mimicking the *in vivo* environments of human cells. With this being said, proper 3D architectures are particularly important to the cell types presented in the connective tissues or sensitive to the mechanical stresses, such as fibroblasts, epithelium, and cancer cells [8]. Take tumours as an example, cancer cells have shown different sensitivities towards their microenvironments at both the initial development stage and late metastasis [4, 9]. Previous studies have shown that stimulation of the ECM in 3D culture with selective incorporation of adhesion factors and signalling factors is capable of turning the epithelia carcinoma cells into non-cancerous cells [4, 10–12]. Such cells have also shown a relatively high degree of drug resistance compared to their counterparts cultured in conventional 2D models. Collectively, these observations highlight the critical need of 3D culture models that may replicate the *in vivo* cell–cell interactions and ECM deposition. Towards this end, the so-called multicellular tumour spheroids, which are microscale cell clusters formed by self-assembly [13, 14], have proven to resemble *in vivo* tumours in many aspects, including growth kinetics, metabolic rates, and resistance to antitumor therapies [15]. For instance, multicellular tumour spheroids mimic *in vivo* tumour-like development patterns of avascular tumour nodules with respect to morphology and growth kinetics [16]. In addition, xenograft tumour sections from the nude mice and tumour spheroids appear to have similar hematoxylin and eosin staining [17].

Currently available strategies for the generation of spheroids can be broadly categorized into matrix-assisted assembly and device-assisted assembly [18]. Commonly used matrices to assist 3D cell culture include naturally derived and synthetic biomaterials, such as collagen, alginate and Matrigel. Cells encapsulated in these matrices have shown loss of polarity, which is a hallmark of cancer. However, most of the bio-matrices suffer from xenobiotics. Furthermore, these synthetic or naturally derived biomatrices are often heterogeneous in compositions and the quality may vary from batch to batch [19]. The device-assisted assembly is normally performed by culturing in suspension (such as rotating bioreactors and hanging drops), or by the use of non-adhesive surfaces [20]. Take the culture in the ultra-low attachment plate (ULAP) for example, cells are unable to attach on the surface, and thus aggregate into a single spheroid spontaneously, negating the undesirable mechanical stress provided by the bio-matrices. The approach of ULAP is relatively accessible and easy, but is limited by variation in spheroid size, cell number and shape. To improve the control over the spheroid size, the hanging drop allows cells to aggregate into a single spheroid at the bottom of the small volume of the drop [21]. However, the technique is difficult to scale up and very time consuming [20].

Recently, a multitude of microfluidic systems has emerged as potential solutions for spheroids generations [22]. Although they have shown great potential in providing improved control of spheroid size and cellular composition, most of the existing techniques still relies on assembling the cells with biomatrices [23]. Our previous efforts [24, 25] as well as the work of McMillian *et al* [26] have demonstrated the possibilities of cultivating spheroids in a scaffold-free format in double emulsions and single emulsions, respectively. Culturing cells in single emulsion often suffers from limited nutrient and respiratory gas transport. Therefore, McMillian *et al* introduced a storage array for trapping the single emulsions and subsequent droplet breakage, enabling further cultivation of the initially formed seed spheroids [26]. On the other hand, cultivation in double emulsions represents a flexible approach for sustained culture and subsequent drug studies. However, the generation of double emulsion is challenged by the cumbersome surface treatment process, where the wettability of channel requires spatial control. This is particularly tedious when it comes to modifying the commonly used polydimethylsiloxane (PDMS) from strongly hydrophobic to hydrophilic at selective regions. Previous efforts have achieved differential wettability on one single chip either by photo-patterning the to-be-wetted areas [27] or by confining the reactive coating materials to specified regions in the microchip [28]. Our previously developed two-chip approach [29] has rendered an easy operation, however, additional connection is required between the two chips.

In this study, a novel strategy, taking advantages of the 'airway resistance', is introduced to selectively treat the surfaces of PDMS, which has shown robust performance in changing the wettability of PDMS at the designated region in a facile manner. Enabled by this technology advancement, the generation of double emulsions becomes relatively easy and user-friendly. To demonstrate the applicability of this approach, two human colorectal carcinoma epithelial cell lines, Caco-2 and HT-29, were introduced and cultivated in the double emulsions. The formation of spheroids with both cell types were initiated without additional supplement in the double emulsions. As a pioneering effort to investigate the molecular characteristics of the double-emulsion generated spheroids, the activities of human topoisomerase I (hTopI), dependent on the differentiation level of cells, were measured by an ultrasensitive approach based on DNA nanosensors. The

measured results were compared with the activities of cells cultivated in conventional 2D culture model and 3D ULAP model. At the molecular level, enhanced hTopI activities were observed in the 3D culture models, when compared to the 2D culture, which suggests an altered differentiation level for the cells cultured in 3D, particularly the cells cultured in double emulsions. Furthermore, immunostaining of E-cadherin and lgr5 indicates drastic different patterns in the ECM arrangement and the distribution of self-renewal stem cells between the 3D and 2D culture models. Nonuniformity was observed in ULAP, which may present a major challenge in the assessment of drug responses using ULAP as an *in vitro* model. These observations collectively support that the double emulsions provide enhanced control to the spheroid production by having each emulsion as an individual cell incubator for spontaneous cell assembly. With the burden eased by the proposed airway resistance based surface treatment, double emulsions may become a user-friendly format for 3D cell culture. Furthermore, the developed DNA nanosensor is expected to advance our understanding of the molecular characteristics of multicellular spheroids.

Materials and methods

Design and fabrication of chip

The microfluidic chips were designed based on the flow-focusing geometry [29, 30] as shown in figure 1(a), with 100 μm in width for the main channel and 40 μm in width for the nozzle throat. The water-in-oil (W/O) single emulsions were generated at the first cross-junction (figure 1(b)), while the single W/O emulsions were dispersed into the water phase at the second cross-junction, forming the water-in-oil-in-water (W/O/W) double emulsions with a thin oil layer (figure 1(c)). The chips were fabricated by the conventional soft lithography process [31]. Briefly, the patterns were designed and printed on a transparency in a resolution of 25 400 DPI (CAD/Art Services, Bandon, OR, USA). The patterns were then transferred onto a silicon wafer coated with negative photoresist SU-8 3050 following the manufacturer's protocol, which produced a SU-8 master mold of 80 μm high (MicroChem, Westborough, MA, USA).

Polydimethylsiloxane (PDMS) pre-polymer and a cross-linker (Sylgard 184 Silicon Elastomer Kit, Dow Corning, Midland, MI) were fully mixed at a ratio of 10:1. The mixture was then poured on top of the patterned SU-8 master mold and degassed to remove bubbles. After curing at 65 °C for 1 h, the cured PDMS chip was peeled off from the SU-8 master mold. The inlet and outlet ports were punched as through holes using a hole-puncher (PDMS Biopsy Puncher, 1.25 mm, KPUNCH125, ELVEFLOW, France). Both the PDMS chip and a 1 mm thick PDMS slab were treated by O_2 plasma for 30 s (RF power: 30 W, O_2 flow: 20 sccm, Vision 320 RIE, Advanced Vacuum, Sweden). Immediately after the plasma treatment, the PDMS chip was bonded to the 1 mm thick PDMS slab to completely seal the microchannels (figure 1(d)).

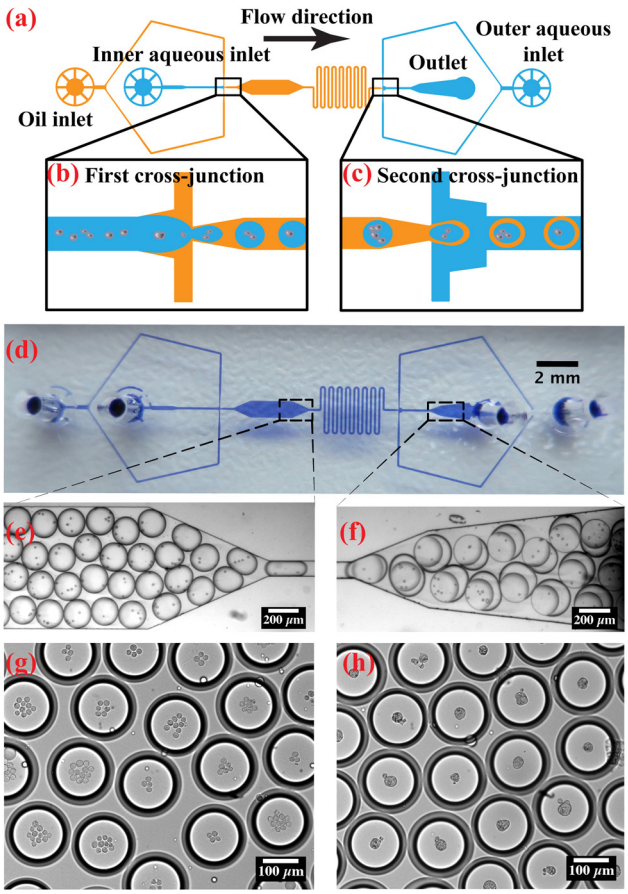

Figure 1. Generation of homogeneous double emulsions. (a) Schematic illustration of the designed microfluidic device utilized in this study. (b) At the first cross-junction, cells are encapsulated into water-in-oil single emulsions. (c) At the second cross-junction, single emulsions are further dispersed into double emulsions with thin oil shells. (d) The overview of the fabricated PDMS chip. (e) Single emulsions with intestinal cells encapsulated. (f) Double emulsions generated after the second cross-junction. (g) Intestinal cells distributed in double emulsions at day 0. (h) Intestinal cells forming multicellular spheroids in double emulsions after 24 h cultivation.

Selective surface modification of PDMS chip

To disperse W/O single emulsions into water phase forming double-emulsions, the wettability of PDMS channels in the second cross-junction and the outlet (illustrated in blue, figure 1(a)), was modified to be hydrophilic. To render the selective surface modification, an 'airway resistance' was introduced in the serpentine region of the microchannel, so that the chemicals utilized for surface treatment would be confined in second cross-junction. The chemistry of a two-step benzophenone initiated acrylic acid-polymerization [32] was adopted to modify the wettability of PDMS. The generation of 'airway resistance' was operated as illustrated in figure 2. Briefly, a slug of water solution was introduced from the inner aqueous inlet and the oil inlet, up till the serpentine region (blue region, figure 2(a)). Subsequently, 10% of benzophenone in acetone was introduced into the chip from outer aqueous inlet to outlet by capillary force spontaneously, leaving an air plug in the middle of the chip (marked

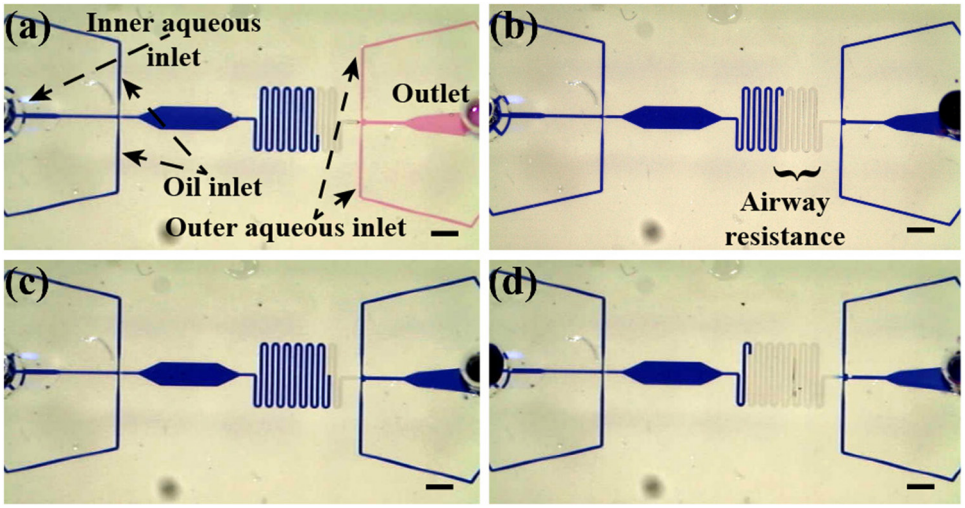

Figure 2. Principle of the 'airway resistance' rendered selective surface treatment. (a) Slug of liquid was introduced from the inner aqueous inlet and the oil inlet, up till the serpentine region (blue region on the left). Subsequently, the benzophenone in acetone was driven from outer aqueous inlet to the outlet by capillary force spontaneously (incarnadine region on the right), leaving a small air plug in between the two liquid phases. (b) After removing the acetone solution (incarnadine region on the right in (a)), washing fluid or another segment of aqueous solution (coloured in blue) could be injected from the outlet and only reached the second cross-junction region, due to the blocking of 'airway resistance'. (c) Minimal airway resistance, generated by introducing extended amount of liquid from the inner aqueous inlet. (d) Elongated airway resistance, generated by introducing reduced mount of liquid from the inner aqueous inlet. Both the conditions of (c) and (d) have demonstrated effective surface treatment, showing the robustness of the proposed design. Scale bar: 1 mm.

in incarnadine, figure 2(a)), due to the high resistance produced by the serpentine structure. The solution was then left for 30 s, followed by a washing step with water for 2 min. Subsequently, a mixture of 10% acrylic acid monomer, 1 mM $NaIO_4$, and 0.5% benzyl alcohol in water, was applied into the benzophenone-initiated regions, in the same manner as mentioned above. The chip was then exposed to UV light (UV-Exposure box, 32 W, Gie-Tec GmbH, Eiterfeld, Germany) for 5 min, rendering the surface hydrophilic for the treated regions. The treated PDMS chips were then cleaned by water, air dried and stored for future use.

Cell lines and cell culture

Two human colorectal carcinoma epithelial cell lines, Caco-2 cell line and HT-29 cell line were seeded in T175 cm^2 flasks and grown in complete medium (minimum essential media (MEM), supplemented with glutaMAX (Gibco), 20% fetal bovine serum (FBS), 100 IU ml^{-1} penicillin, 100 μg ml^{-1} streptomycin, and 1% non-essential amino acid (Sigma-Aldrich). When the cells were 80% confluent, they were trypsinized and transferred into different culture environments, i.e. 2D culture in 6-well plates (Corning), 3D culture in ultra-low attachment plate (ULAP, 6-well plate, Corning), and 3D culture in double-emulsions, for 2 d cultivation. All cell lines used in the experiments were between the passage 6 to passage 15. The seeding density was kept at 3×10^5 cells per well for both the 2D and 3D culture in a 6-well plate. For cultivation in double emulsions, cells were suspended to a concentration of 5×10^6 cells ml^{-1} and introduced into a 1 ml syringe (Becton Dickinson and Company) for double emulsion encapsulation as elaborated in the following section.

Cell encapsulation in double-emulsions

Three flow phases were prepared for the cell encapsulation: inner aqueous, middle oil, and outer aqueous, containing cells in the complete culture medium, biocompatible fluorocarbon oil HFE-7500 with 1% Pico-surf (Dolomite Microfluidic, USA), and the complete culture medium with 2.5% pluronic F-127 (Sigma), respectively. The aqueous solutions and oil were loaded into commercially available syringes (1 ml or 3 ml, luerlok, BD), which were connected to tygon microbore tubing (ID: 0.51 mm, OD: 1.52 mm, Cole Parmer) through syringe adaptors (23 gauge, KelF Hub, Hamilton Company).

Three syringe pumps (PHD2000, Harvard Apparatus, Holliston, MA) were used to control the flow rates of the inner aqueous phase (9 μl min^{-1}), the middle oil phase (6 μl min^{-1}), and the outer aqueous phase (10 μl min^{-1}), independently. The generated double-emulsions containing cells were collected in eppendorf tubes, transferred to a T75 cm^2 culture flask, and kept in culture in the complete culture medium.

Immunostaining

Prior to the staining, gelatin-coated microscope slides were prepared by dipping the slides quickly into a filtered water solution containing 0.5% gelatin and 1 mM chromium potassium sulfate. The slides were then air-dry at room temperature for future use. Cells from 2D culture (6-well plate) and 3D culture (ULAP and double emulsions) were fixed by 4% paraformaldehyde (PFA) in PBS for 10 min, and then washed twice with PBS. A drop of fixed cells was smeared on the gelatin-coated microscope slide. When the smears were almost dried, washed the slides containing the fixed cells with PBS

and subsequently with the blocking buffer containing 0.5% BSA in PBS for 30 min at room temperature. The specimen, the fixed cells on slides, was then incubated with primary antibody (anti-E-cadherin, 1:100, Cell Signaling Technology Inc., USA) for 2 h at 4 °C, washed by 0.5% BSA in PBS and followed by secondary antibody (FITC-coupled anti rabbit IgG, 1:400, Cell Signaling Technology Inc., USA) and another primary antibody (PE-coupled anti-lgr5, 1:10, Miltenyi Biotec) for 1 h at 4 °C. The specimen was subsequently incubated with Hoechst33342 (1:10 000, Sigma) for 5 min. The immunostaining was done in the dark.

Measurement of hTopI activities

The hTopI activities was measured via a DNA nanosensor, following the previously developed technique, termed rolling circle-enhanced enzyme activity detection (REEAD) [33]. Firstly, nuclear extraction was acquired by incubating the cells with 1 ml of lysis buffer (0.1% Igepal CA-630, 10 mM Tris-HCl (pH 7.9), 10 mM $MgCl_2$, 15 mM NaCl and 1% phenylmethyl sulfonyl fluoride (PMSF)) on ice for 10 min. Subsequently, lysates were spun at 400 g for 5 min and the supernatant was removed. 50 μl of nuclear extraction buffer (0.5 M NaCl, 20 mM HEPES (pH 7.9), 20% glycerol and 1% PMSF) was added to the cell pellet and incubated at 4 °C for 1 h. The debris was then spun down at 11 200 g for 10 min. The supernatant was collected as the nuclear extract.

The nuclear extract was then incubated with 0.2 μM of dumbbell DNA substrates (figure 4(a)) (DNA Sequence: 5′-A GAA AA ATT TTT AAA AAA ACT GTG AAG ATC GCT TAT TTT TTT AAA AAT TTT TCT AAG TCT TTT AGA TCC CTC AAT GCT GCT GCT GTA CTA CGA TCT AAA AGA CTT AGA-3′), in the hTopI reaction buffer (10 mM Tris-HCl (pH 7.5), 5 mM $CaCl_2$, 5 mM $MgCl_2$, 10 mM DTT and 0.2 μg μl^{-1} bovine serum albumin (BSA)) for 60 min at 37 °C, followed by a heat inhibition at 65 °C for 20 min. The samples were then placed onto the primer pre-conjugated microscopic slides, where the circularized products were able to hybridize to. The hybridization was done at 20 °C–25 °C for 60 min. The slides were then washed for 2 min at 20 °C–25 °C in a washing buffer (100 mM Tris-HCl (pH 7.5), 150 mM NaCl and 0.3% SDS), followed by a wash in second washing buffer (100 mM Tris-HCl (pH 7.5), 150 mM NaCl, and 0.05% Tween-20) for 2 min at 20 °C–25 °C. Dehydration of slides was performed by incubating the slides with 96% ethanol for 1 min followed by air dry.

The slides were then subjected to the so-called Rolling Circle Amplification (RCA), performed in 1× Phi29 buffer supplemented with 0.2 μg μl^{-1} BSA, 250 μM dNTP and 1 unit μl^{-1} Phi29 DNA polymerase in a 3 μl reaction mixture. The reaction was stopped by repeating the wash steps as above-described. The final elongated products were recognized by hybridizing with 0.2 μM ID33-FAM detection probe in a hybridization buffer (20% formamide, 2× SSC buffer and 5% glycerol) in a 5 μl reaction mixture for 30 min at 37 °C. Finally, the slides were washed and mounted with a piece of coverslip by Vectashield antifade mounting medium (Vector Laboratories, Burlingame, CA, USA).

Microscopy and image analysis

Processes of cell encapsulation and double emulsion formation were monitored and documented with a microscope (4X Plan Achromat Objective, NA = 0.1, CKX41, Olympus) and an industrial camera (PL-B742F, Pixelink). Fluorescence analyses, including the immunostaining and REEAD measurements, was performed by analyzing the slides with Olympus IX73 epifluorescence microscope equipped with an Uplsapo 60 oil objective (NA = 1.35). Images were acquired by the Andor Zyla sCMOS camera operated by Olympus cellSens™ Dimension. For the measurements of hTopI activities, 20 images were recorded for each experiment, images were analyzed with ImageJ software and fluorescent spots were quantified by the tool of analyze particles. The statistical significance was determined using Prism 5.0 (GraphPad Software, La Jolla, CA, USA).

Results and discussion

Chip design and selective surface treatment

To satisfy the request of facile surface treatment of PDMS selectively, this study proposes a novel design, which is composed of two cross-junctions and a serpentine structure in between, as shown in figure 1(a). The cross-junctions and the serpentine structure are designed to render the dispersion of W/O/W double emulsion and sufficient airway resistance for the selective surface treatment, respectively. Previously developed two-step benzophenone initiated acrylic acid-polymerization was utilized to alter the wettability of PDMS [32]. The catalytic chemical reaction was restricted in selected regions (coloured in blue, figure 1(a)), taking advantages of the high resistance produced by the serpentine structure.

The operation of the ‘airway resistance’ rendered selective surface treatment is illustrated in figure 2 (see also the supplementary video) (stacks.iop.org/JMM/27/095014/mmedia). Firstly, a slug of liquid was introduced from the inner aqueous inlet and the oil inlet, up till the serpentine region (blue region, figure 2(a)). Subsequently, the benzophenone in acetone was driven from the outer aqueous inlet to the outlet by capillary force spontaneously (incarnadine region, in figure 2(a)), leaving a small air plug between the two liquid phases. After the initiation by benzophenone, the benzophenone/acetone solution could be removed without infiltration to the serpentine region and the first cross-junction. Following the same principle, washing fluid and the aqueous solution containing the acrylic acid monomers could be injected from the outlet. Thereby it only reached the second cross-junction (shown as the blue region on the right, figure 2(b)). Empirical validation suggested that when the flow resistance of the serpentine structure was sufficiently high, the airway resistance would be able to resist the flow from entering the first cross-junction. Given that the hydrodynamic resistance is proportional to the channel length while the cross-section of the channel remains uniform [34], the resistance of the serpentine region (34.7 mm) was design to be around 17 times higher than the resistance from the second cross-junction to the outer aqueous

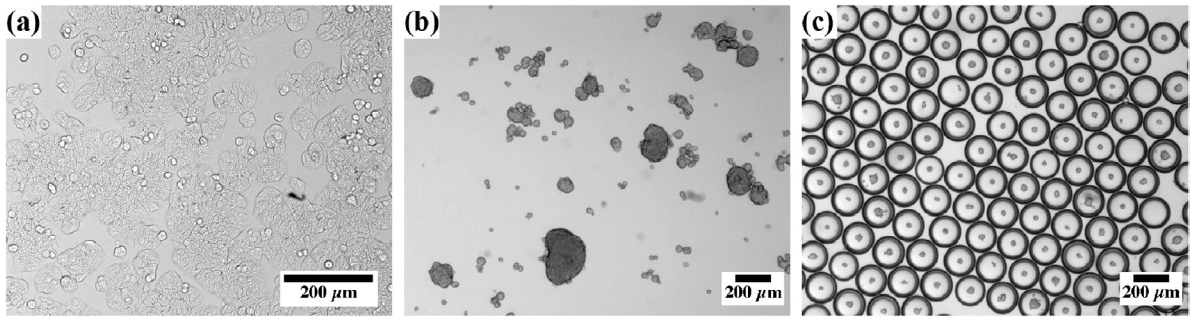

Figure 3. HT-29 cells cultured for 24 h in different formats. (a) 2D culture in conventional 6-well plate, (b) 3D culture in ultra-low attachment plate (ULAP), and (c) 3D culture in double emulsions. Scale bar: 200 μm.

inlet (1.96 mm), to ensure that the flow would only move from the outer aqueous inlet to the outlet. Employing this robust and facile strategy, the designated regions were rendered hydrophilic. Surface hydrophilicity was confirmed by a separate experiment measuring the water contact angle on a flat PDMS slab, which changed from 105°–70° after the treatment (data not shown).

The 'airway resistance' is crucial to restrain the fluid from entering the serpentine region. One may wonder how much of the air plug is required in order to generate sufficiently high resistance. To demonstrate the undemanding request for the operation, two extreme cases, as illustrated in figures 2(c) and (d), were performed by introducing extended and reduced amount of liquid from the inner aqueous inlet, which produced minute (1 loop) and sizable (7 loops) airway resistance, respectively. In both cases, the flow from the outer aqueous inlet was successfully directed to the outlet in both cases without disturbing the flow in the serpentine region.

Generation of double emulsions and cell encapsulation

As shown in figures 1(b) and (e), an aqueous phase containing cells was dispersed into the W/O single emulsion droplets. The single emulsions were then entering the observation window, passing the serpentine channel, and subsequently dispersed by the outer aqueous at the hydrophilic second cross-junction, forming W/O/W double emulsions (figures 1(c) and (f)). Note that the size and structure of both the single emulsions (figure 1(e)) and double emulsions (figure 1(f)) remained homogeneous and stable. Distribution of cells in each emulsion followed the Poisson distribution, as reported previously [25]. Double emulsions collected directly from the outlet were shown in figure 1(g). The double emulsions were then kept in culture flasks containing proper culture medium. After 2 d of cultivation, the cells were observed to self-assemble into multicellular spheroids (figure 1(h)) without any biomaterial scaffolds. The spontaneous clustering of cells is most likely due to the strong cell-cell interaction in the confined environment.

Cells cultured in 2D and 3D

In our previous study [25], we have shown successful spheroid formation using PMEF (primary mouse embryo fibroblasts), HepG2 (liver hepatocellular carcinoma), and human mesenchymal stem cell (hMSC). In this study, we explore the molecular characteristics of the double emulsion using two types of intestinal cells, Caco-2 and HT-29. Furthermore, this study intends to explore the molecular and morphological characteristics of the cells cultured in different conditions, namely 2D in normal culture plate, 3D in ULAP, and the described double emulsion setup. Figure 3 shows representative results obtained when HT-29 cells were cultured using each of the above-mentioned culturing formats for 48 h. As expected, HT-29 cells formed monolayer colonies (figure 3(a)) in the 2D culture format, and tended to cluster into multicellular spheroids in the 3D culture formats, i.e. ULAP (figure 3(b)) or double emulsions (figure 3(c)). It is of particular note that the spheroids were observed to be homogeneous in size under the culture in double emulsions (figure 3(b)), as compared to in ULAP (figure 3(b)). Moreover, no significant difference in proliferation, estimated by counting the cell numbers, was perceived between the cultures of ULAP and double emulsions. Assuming similar proliferation rate in both double emulsion and ULAP, this observation implies that the large spheroids observed in ULAP are probably due to large amount of cells, which initiate the aggregation randomly, or due to secondary aggregations between several small seed spheroids.

Enzymatic activities of cells cultured in 2D and 3D

hTopI is involved in many cellular processes such as replication, transcription and chromatin remodeling [35, 36]. Therefore, the activity and expression of hTopI are anticipated to be highly dependent on the cell status. The activities of hTopI have been previously shown altered during differentiation of Caco-2 cells [37]. As the first attempt to investigate whether the differentiation level of cells may be changed by the culture format, hTopI activities were quantified via DNA nanosensors by the previously established rolling circle-enhanced enzyme activity detection (REEAD) assay, with the working principle shown in figure 4(a) [33]. For both Caco-2 (figure 4(c)) and HT-29 (figure 4(d)), higher hTopI activities were observed in the groups of ULAP and double emulsions, when compared to the 2D culture. However, further analysis suggested that only the results obtained when analysing cells cultivated in double emulsions presented statistical significant difference to the results obtained when analysing cells grown in the 2D culture. This is because the results obtained for the groups of

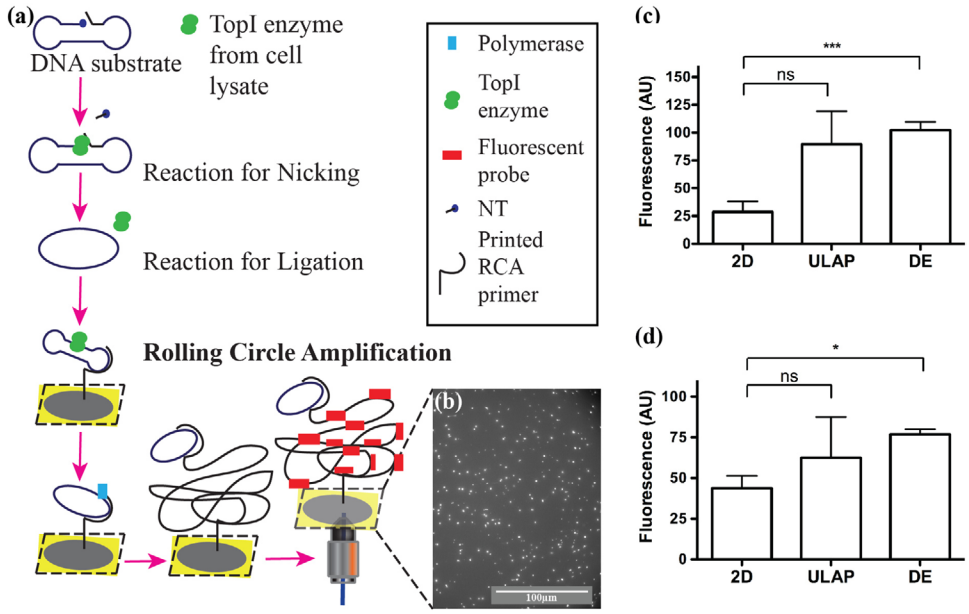

Figure 4. Measurement of human topoisomerases I (hTopI) activities based on rolling circle-enhanced enzyme activity detection (REEAD). (a) REEAD is conducted essentially as previously described [33]. Briefly, hTopI enzymes react upon on the specifically designed DNA substrate, turning the linear substrate into a circle. Subsequently, polymerase (blue square) is able to extend the surface conjugated primer into a DNA tandem through the so-called rolling circle amplification (RCA) reaction. Fluorescent probes (red rectangle) are then used to 'light up' the amplified DNA. (b) Representative result showing the fluorescent spots, which indicates individual hTopI activity. (c) Results from Caco-2 cells cultured in 2D, ULAP and double emulsions (DE). (d) Results from HT-29 cells cultured in 2D, ULAP and DE. The results are presented as the mean of three individual experiments normalized to a positive and negative control, while the error bar represents the standard error of the mean. Significant difference is determined by unpaired *t*-tests (ns: no significance, $^{*}p < 0.02$, $^{***}p < 0.001$).

double emulsions presented smaller errors compared to the ones obtained for ULAP groups. Collectively, these evidences suggest a change in the differentiation patterns when cells are clustered into spheroids. The small variations observed in double emulsions further support that double emulsions provide a homogeneous condition to cultivate 3D multicellular spheroids and the subsequent studies.

Analyses of differentiation biomarkers

Further analysis was conducted by immunostaining of selected differentiation markers using both Caco-2 and HT-29 cultivated in 2D, ULAP, and double emulsions for 2 d. E-cadherin was used to assess the ECM arrangement, whereas the lgr5 served as an indicator of self-renewal stem cell. As shown in figures 5(a) and (b), both HT-29 and Caco-2 cells cultivated in 2D conditions developed strong E-cadherin signals between each cells and weak but homogeneous expression of the lgr5 signal. On the other hand, in cells cultured in either 3D culture conditions, expression of E-cadherin was only observed around the edge of each spheroid. In some tissue-like spheroids, single concentrated lgr5 positive signals were detected for both HT-29 and Caco-2 (figures 5(c)–(f)). The lgr5 positive cells, serving as self-renewal stem cells, play a critical role in building crypt-villus structures of intestinal epithelium [38, 39]. The lgr5 positive cells along with the observed E-cadherin around the spheroids observed in the 3D culture formats suggests that the cell aggregation is produced with a rather natural polarity, which may serve as a foundation to initiate intestinal organoids *in vitro*.

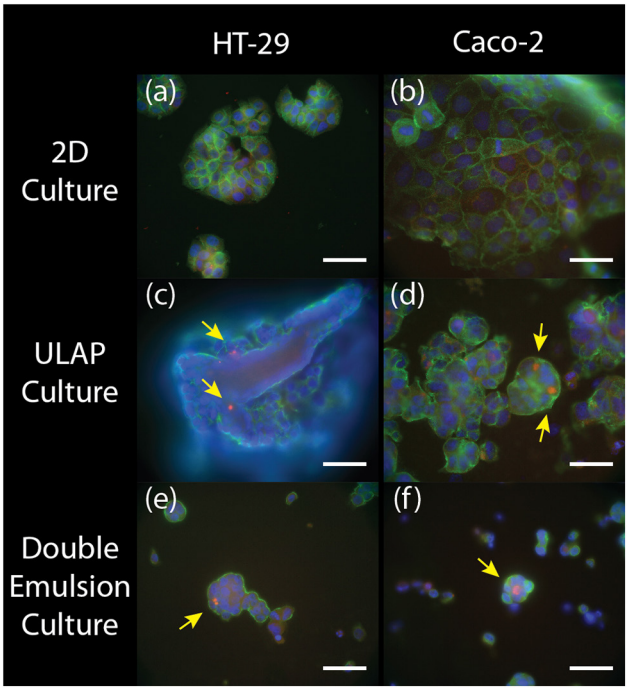

Figure 5. Fluorescent immunostaining of HT-29 and Caco-2 cells. (a) HT-29 cells and (b) Caco-2 cells cultured in conventional 6-well plate (2D), (c) HT-29 cells and (d) Caco-2 cells cultured in ultra-low attachment plate (ULAP), and (e) HT-29 cells and (f) Caco-2 cells cultured in double emulsions. Immunostaining was performed after 48 h cultivation. Nucleus (blue), E-cadherin (green), and lgr5 (red). Arrows showing where the concentrated lgr5 positive signals were observed. Scale bar: 50 μm.

Although similar phenomena were observed in cells cultivated in either ULAP or using double emulsions, major differences were observed in the patterns of lgr5 positive cells and E-cadherin expression. The lgr5 positive cells were randomly distributed in each cell aggregation for ULAP, whereas single lgr5 positive cells were observed in each spheroid for double emulsions. The expression of E-cadherin was found in cells located inside the spheroids formed in ULAP, as opposed to double emulsions formed spheroids in which E-cadherin expressing cells were only observed at the edge. These observations indicate that the spheroids cultured in ULAP may initiate from more than one seed organoid, assuming singular polarity where each seed organoid only has one single lgr5 positive stem cell. Seed organoids formed in ULAP may adhere to each other randomly and further aggregate into a huge spheroid as shown in figures 5(c) and (d).

The spheroid formation in double emulsion is rapid, typically within 2 h. However, with limited nutrient in the double emulsions, the spheroids have shown normal growth for up to 4 d [25]. Our previous study has demonstrated a sustained culture of double emulsion-formed spheroids for up to 7 d, given the oil layer is removed [25], which may pose a concern for the application of tissue engineering. In this study, we switch the gear to investigate the seed spheroids when the crypt-villus structures are initially formed, as indicated by the lgr5 expression. Indeed, the molecular and morphological features of the seed spheroids are both observed more uniform than the ULAP generated counterparts. We envision that the uniform culture environment offered by the double emulsion may present a reliable *in vitro* model for the assessment of drug responses using seed spheroids mimicking early tumorigenesis.

Conclusions

The 3D architecture of multicellular cancer spheroids is considered a more valid *in vitro* simulation of the *in vivo* tumour. Although many innovations have been proposed to produce and cultivate multicellular cancer spheroids, challenges remain in the tedious procedures and the lack of consistency. As a continuous advancement of our previous effort, this study presents a novel approach to selectively modify the wettability of PDMS, by the introduction of airway resistance. Made possible by this robust surface treatment, two model intestinal cancer cell lines have observed clustered into the spheroids in a scaffold-free format. Further characterization of the generated spheroids has shown characteristics similar to those cultivated in a well-established 3D model, i.e. ultra-low attachment plates. This study also presents the first measurement of topoisomerase activities enabled by our previously developed DNA nanosensors. Evidenced by the obtained results, the spheroids produced in double emulsions are consistent in not only their sizes, but also their molecular and functional characteristics. Further investigations of the generated spheroids with different cells types are expected to open up new possibilities in promoting the spheroids models for cancer study.

Acknowledgments

The authors would like to acknowledge the support from the CUHK start up fund, the Lundbeck Foundation (R95-A10275), the Dagmar Marshalls Fond, the Arvid Nilssons Fond, Krista og Viggo Petersens Foundation, Kleinsmed Sven Helge Arvid Schrøders og Hustrus Foundation, and Aage and Johanne Louis-Hansens Foundation.

ORCID iDs

Yi-Ping Ho https://orcid.org/0000-0002-2052-9724

References

[1] Abbott A 2003 *Nature* **424** 870–2
[2] Cukierman E, Pankov R, Stevens D R and Yamada K M 2001 *Science* **294** 1708–12
[3] Petrie R J, Koo H and Yamada K M 2014 *Science* **345** 1062–5
[4] Weaver V M, Petersen O W, Wang F, Larabell C A, Briand P, Damsky C and Bissell M J 1997 *J. Cell Biol.* **137** 231–45
[5] Nelson C M and Bissell M J 2006 *Annu. Rev. Cell Dev. Biol.* **22** 287–309
[6] Mammoto A, Mammoto T and Ingber D E 2102 *J. Cell Sci.* **125** 3061–73
[7] Ingber D E 1993 *Cell* **75** 1249–52
[8] Pampaloni F, Reynaud E G and Stelzer E H 2007 *Nat. Rev. Mol. Cell Biol.* **8** 839–45
[9] Wolf K, Mazo I, Leung H, Engelke K, von Andrian U H, Deryugina E I, Strongin A Y, Brocker E B and Friedl P 2003 *J. Cell Biol.* **160** 267–77
[10] Chen L, Xiao Z, Meng Y, Zhao Y, Han J, Su G, Chen B and Dai J 2012 *Biomaterials* **33** 1437–44
[11] Gurski L A, Jha A K, Zhang C, Jia X and Farach-Carson M C 2009 *Biomaterials* **30** 6076–85
[12] Lee M Y, Kumar R A, Sukumaran S M, Hogg M G, Clark D S and Dordick J S 2008 *Proc. Natl Acad. Sci. USA* **105** 59–63
[13] Achilli T M, Meyer J and Morgan J R 2012 *Expert Opin. Biol. Ther.* **12** 1347–60
[14] Haycock J W 2011 *Methods Mol. Biol.* **695** 1–15
[15] LaBarbera D V, Reid B G and Yoo B H 2012 *Expert Opin. Drug Discov.* **7** 819–30
[16] Friedrich J, Seidel C, Ebner R and Kunz-Schughart L A 2009 *Nat. Protocols* **4** 309–24
[17] Ma H L, Jiang Q, Han S, Wu Y, Cui Tomshine J, Wang D, Gan Y, Zou G and Liang X J 2012 *Mol. Imaging* **11** 487–98
[18] Xu X, Farach-Carson M C and Jia X 2014 *Biotechnol. Adv.* **32** 1256–68
[19] Liu Z and Vunjak-Novakovic G 2016 *Curr. Opin. Chem. Eng.* **11** 94–105
[20] Lin R Z and Chang H Y 2008 *Biotechnol. J.* **3** 1172–84
[21] Tung Y C, Hsiao A Y, Allen S G, Torisawa Y S, Ho M and Takayama S 2011 *Analyst* **136** 473–8
[22] Kwapiszewska K, Michalczuk A, Rybka M, Kwapiszewski R and Brzozka Z 2014 *Lab Chip* **14** 2096–104
[23] Sabhachandani P, Motwani V, Cohen N, Sarkar S, Torchilin V and Konry T 2016 *Lab Chip* **16** 497–505
[24] Ma X, Jepsen M L, Ivarsen A, Nygaard J V, Tesauro C, Knudsen B R and Ho Y P 2016 *The 20th Int. Conf. on Miniaturized Systems for Chemistry and Life Sciences (Dublin, Ireland, 9–13 October 2016)*
[25] Chan H F, Zhang Y, Ho Y P, Chiu Y L, Jung Y and Leong K W 2013 *Sci. Rep.* **3** 3462

[26] McMillan K S, Boyd M and Zagnoni M 2016 *Lab Chip* **16** 3548–57
[27] Schneider M H, Willaime H, Tran Y, Rezgui F and Tabeling P 2010 *Anal. Chem.* **82** 8848–55
[28] Abate A R, Thiele J, Weinhart M and Weitz D A 2010 *Lab Chip* **10** 1774–6
[29] Zhang Y, Ho Y P, Chiu Y L, Chan H F, Chlebina B, Schuhmann T, You L and Leong K W 2013 *Biomaterials* **34** 4564–72
[30] Baroud C N, Gallaire F and Dangla R 2010 *Lab Chip* **10** 2032–45
[31] Qin D, Xia Y and Whitesides G M 2010 *Nat. Protocols* **5** 491–502
[32] Wang Y, Lai H H, Bachman M, Sims C E, Li G P and Allbritton N L 2005 *Anal. Chem.* **77** 7539–46
[33] Stougaard M, Lohmann J S, Mancino A, Celik S, Andersen F F, Koch J and Knudsen B R 2009 *ACS Nano* **3** 223–33
[34] Fox R W and McDonald A T 1994 *Introduction to Fluid Mechanics* (New York: Wiley)
[35] Champoux J J 2001 *Annu. Rev. Biochem.* **70** 369–413
[36] Leppard J B and Champoux J J 2005 *Chromosoma* **114** 75–85
[37] Ulukan H, Muller M T and Swaan P W 2001 *Int. J. Cancer* **94** 200–7
[38] Barker N *et al* 2007 *Nature* **449** 1003–7
[39] Sato T *et al* 2009 *Nature* **459** 262–5